Sensing and Bio-Sensing Research 19 (2018) 7–13

Contents lists available at ScienceDirect

Sensing and Bio-Sensing Research

journal homepage: www.elsevier.com/locate/sbsr

A novel technique for detection of biomolecules and its aqueous concentration using a double gate graphene field effect transistor

Prattay D. Kairy*, Mustafizur Rahman, Emran Khan Ashik, Quazi D.M. Khosru

Department of Electrical and Electronic Engineering, Bangladesh University of Engineering and Technology, Dhaka 1000, Bangladesh

1. Introduction

Biosensor is a device combining an aqueous solution containing biomolecules and a detector element (electrical transducer) that generates an electrical signal proportional to the concentration of the biomolecules in the analyte. Since the invention of graphene [1] and advancements towards inorganic transition metal dichalcogenides inspired by remarkable characteristics of graphene [1,2], the performance of biosensors has been improving with the same trend [3–8]. Recently, graphene and graphene-based devices especially field effect transistors (FETs) have become a matter of interest for the use in nanobiosensors. Since the introduction of graphene to carbon electronics, it has bought a new excitation to field effect transistors replacing the traditional channel material to bring about a great amelioration to device characteristics beyond traditional CMOS technology [9,10] but two-dimensional graphene being a zero band gap material, makes it unsuitable for transistor applications [11]. However, energy gap can be induced by means of lateral confinement [12] by making the sheet into nanotube, nanowire or maybe nanoribbon to confine the carrier movement in one dimension. The exceptionally excellent carrier transport properties [13] of graphene nanostructure FETs allured profound interests of the researchers in the way of developing carbon-based nanostructures.

Use of graphene in nanobiosensor provides two major advantages. One corresponds to the fact that it does not contain metallic impurities, and so, does not interfere with material electrochemistry [3]. Moreover, graphene has a high surface area which helps to provide desired sensitivity for biosensing system [14,15]. Its strong chemical and physical properties against electrochemical environments make graphene a more suitable for biosensing [16–18].

Yasuhide Ohno et al. [17] have detected pH and protein adsorptions through the help of electrolyte gate field effect transistor (FET) replacing typical gates of FETs with electrolyte solution of Ag/AgCl and found a linear relationship between conductance and electrolyte pH. Park et al. [19] have demonstrated ultrasensitive detection of an odorant, amyl butyrate, using flexible and transparent FET-type B-noses while the gate was replaced by liquid. Jieyi Zhu et al. [20] have reported the study of *E. coli* detection by inducing the bacteria on the channel material, Graphene, in the FET and have formulated real-time detection of *E. coli*. Even study of Carbon Nanotube FET based biosensors in reported articles had bioreceptor to grab biomolecules [21] but a technique through keeping the original design of a well-established FET intact is yet to be reported.

Hence, in this work, a novel approach is presented to detect the presence of biomolecules in an aqueous solution and a theoretical calculation for the aqueous concentration of biomolecules using double gated Graphene Nanoribbon Field Effect Transistor (GNR-FET). Generally, a FET is converted into a bio-sensing device by the process of replacement of the metal gate electrode by a biochemically sensitive surface [22]. This surface is usually an analyte-selective membrane or an ion-conductive solution, which is brought into contact with the analyte solution. However, a new technique has been taken in this study that uses the principle of adsorption of biomolecules on the top gate metal. And so, the requirement of bioreceptors is eliminated as the gate metal works as a pseudo-bio receptor which makes this investigation distinctive. The presence of biomolecules will be detected through the measurable change of the transfer curve of the GNR-FET. One important thing is that different types of biomolecules will surely affect the top gate metal differently and in-turns will have varied effect on the transfer curve. However, this work is a proof of concept study where the technique of adsorption of biomolecules on the metal surface of the gate material is considered as an alternative approach of biosensing. Therefore, in this study only the detection of the presence of the biomolecules and calculation of its aqueous concentration is focused. This study finds that the drain current exhibits a significant change in the subthreshold region after the introduction of the biomolecules on the gate surface. This above concept has been used to calculate the aqueous concentration of the biomolecules on the analyte by relating the work of Langmuir in this context.

2. Device structure and Simulation method

The proposed nanobiosensor is a double-gated GNRFET where armchair multilayer graphene nano-ribbon is used as the channel material. In multilayer graphene, there are sub bands and these sub bands contributes to the on state current of the device and this results in higher

* Corresponding author.
E-mail address: ab.kairy09@gmail.com (P.D. Kairy).

https://doi.org/10.1016/j.sbsr.2018.02.004
Received 19 November 2017; Received in revised form 9 February 2018; Accepted 15 February 2018

Table 1
Dimensions of the nanobiosensor.

Component	Dimensions
Top gate	Length: 15 nm
Bottom gate	Length: 15 nm
Top oxide layer	Thickness: 1 nm
Bottom oxide layer	Thickness: 1 nm
Channel	Length: 15 nm Width: 1.87 nm
Source and drain extension	Length:10 nm

on-current than the monolayer graphene in the devices. Nevertheless, the on current decreases in multilayer graphene with increase in interlayer coupling due to the fact that interlayer coupling increases the spacing between the sub bands presents hindering their contribution in on current [23]. Furthermore, it also decreases the bandgap resulting in band to band tunneling which increases off current. However, Non-AB stacking structure have been observed [24] and in this work the interlayer coupling has been considered to zero. Another advantage the multilayer graphene provides that it is more immune to noise [25]. Gold [Au (100)] serves as gate material and the dielectric insulator is a layer of silicon dioxide. The source and drain of the field effect transistor are doped GNR extension (heavily doped with molar fraction of $5e^{-3}$). The source and drain doping density can easily be realized into a more conventional form of cm^{-2} using the following equation:

$$\frac{(\text{dopant/atom}) \times (\text{No.of atom})}{\text{length} \times \text{Width}}$$

where the dopant per atoms is the molar fraction and the length and width can be found from the Table 1.

Table 1 categorizes the dimensions of the device and the values of the parameters used in the simulation procedure.

The biomolecules in the analyte solution diffuse around and eventually, the diffusion process, which has been studied thoroughgoing, [26] brings the biomolecules within 0.3 to 0.4 nm distance from the metal surface which results in adsorption on the gate material [27]. The work-function of the metal changes as an effect of bio-molecular adsorption [28,29]. This variation of work-function is reflected through the change in threshold voltage of the FET device which will be given grounds later in this report. The approach is to detect the presence of biomolecule through monitoring the change in threshold voltage of the FET device (Fig. 1).

In order to perform both as the metal gate and a receptor surface, a metal with high adsorption capability is required. Biomolecular adsorption at aqueous silver interfaces can be found in the literature [30], but, gold has been reported to have excellent biomolecule adsorption characteristics [31] which is favored by most biomolecules for adsorption over silver surface since the expulsion of water molecules in the first solvation layer at the silver interface presents a free-energy barrier that the adsorbate must overcome to make close contact with the silver surface. The presence of this barrier is not seen in a majority of the gold adsorption cases. As a result, the binding of the amino acids to silver is weaker than that seen for gold [31]. Hence this work can surely be said to be valid for amino acids and polypeptides.

Moreover, Au (100) is used where the surface is reconstructed as Au (100) (5 × 1)-hex interface which shows favorable adsorption characteristics over Au (111) and Au (100) (1 × 1). Studies show that for amino acid the potential energy of adsorption onto the Au(100) surface is slightly more preferable than onto Au(111) [28]. Extended research presented that in the case of the Au (100) (1 × 1) interface, the adsorption under aqueous conditions for a range of amino acids is mediated by an interfacial layer of water. In contrast, binding at Au (100) (5 × 1) revealed a preference for direct surface contact, therefore being the most efficient in adsorption of biomolecules [32].

The use of graphene nano-ribbon provides considerable advantages in case of the nanobiosensor even when the top gate material work as the sensing surface. Firstly, high mobility and carrier velocity of graphene and Graphene Nano Ribbon have been demonstrated experimentally [33] which results in ballistic transport in GNRFET. And also, excellent transport properties have been theoretically predicted for structure perfect GNRs [34]. Since the current in the FET depends somewhat proportionally on the mobility of the carrier, GNR results in a high on/off ratio for drain current. As a result, the sub threshold swing is higher for Graphene Nanoribbon FETs and the use of GNR as the channel material will increase the lowest limit that can be detected using the biosensor at a considerable amount. Secondly, channel geometry of GNRFET can be defined by Lithography which offers a better control on the device and also provides better characteristic than Carbon Nano Tube. Although the monolayer graphene as a channel material do suffers from the lower on/off ration and thus inferior in term of characteristic to CNTFET, multilayer graphene as used in this work as the channel material provide the remedy to this problem [35].

For short-channel transistors, for the purpose of precisely modeling the electrostatics and band to band tunneling the only suitable way is a 3-D simulation [36]. It has to be ensured that the potential profile will obey the Poisson equation. The simulation study is based on self-consistent solution of the 3D Poisson-Schrodinger equation with open boundary conditions to model the atomic level quantum transport, within the Non-Equilibrium Green's Function formalism (NEGF) [37].

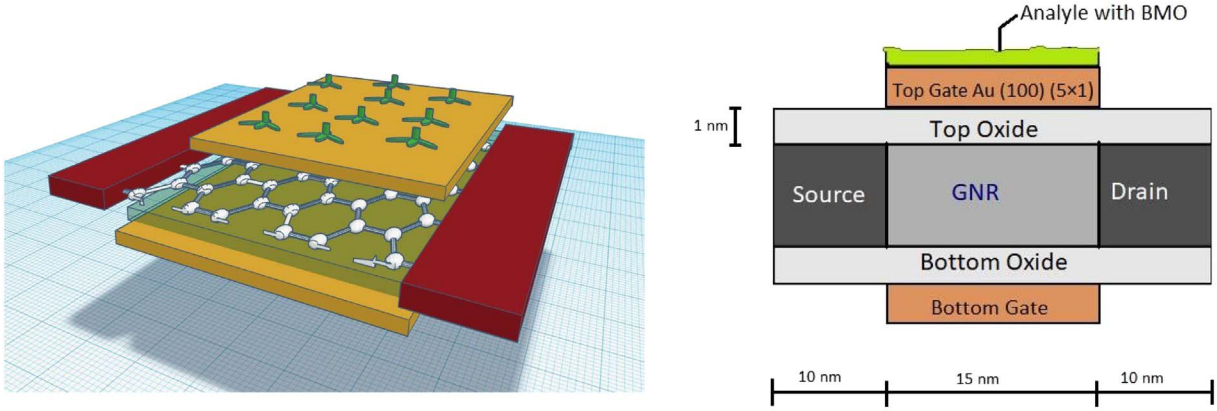

Fig. 1. (a) Proposed biosensor (isometric view). The two yellow portions are top and bottom gate whereas the red rectangles represent the doped extension of GNR. In between the double gates, there exists a channel made of graphene nanoribbon sandwiched between thin layers of dielectric insulator, SiO_2. (b) 2-D view of the sensor for simulation purpose. (For interpretation of the references to colour in this figure legend, the reader is referred to the web version of this article.)

Based on the predictor corrector scheme [38], Newton-Raphson (NR) method of iteration is used to solve the Poisson-Schrodinger equation. By starting from an initial potential, the NEGF equations are solved at the beginning of each NR cycle.

Table 2: Equations used in this work for simulation:

1	Poisson equation	$\nabla[\epsilon(\vec{r})\nabla\varnothing(\vec{r})] = -q\,[p(\vec{r}) - n(\vec{r}) + N_D^+(\vec{r}) - N_A^+(\vec{r})] + \rho_{fix}$	$\varnothing(\vec{r})$ = electrostatic potential $\epsilon(\vec{r})$ = dielectric constant N_D^+, N_A^- = concentration of ionized donors and acceptors ρ_{fix} = fixed charge
2	Current in GNRFET	$I = \frac{2q}{h}\int_{-\infty}^{+\infty} dE\ T(E)[f(E - E_{Fs}) - f(E - E_{FD})]$	q = electron charge T (E) = transmission coefficient f = Fermi-Dirac occupation factor E_{FD}, (E_{FD}) = Fermi level of the source (drain)

For the purpose as the biosensor, by modeling the absorption as the change in work function of the gate metal, the same technique is used to determine the electro statistic characteristics of the sensor. As for typical biosensing application, drain bias is kept very small (V_{DS} = 0.1 V) and doped reservoirs are used as drain and source extensions rather than Schottky contacts as the former results in a much higher on-off ratio of current [39].

3. Results and Discussions

The sensor without any analyte solution is only a GNRFET. After the absorption of biomolecules from the analyte on the gate metal surface, Au [100] to be specific in this case, the sensor device must exhibit a measurable change in the transfer curve of the FET to serve its purpose. Therefore, the original properties of the GNRFET (a short channel transistor) are needed beforehand.

The transfer curve for GNRFET in Fig. 2 shows the Drain current as a function of Top Gate voltage. It is simulated for the chosen gate material, Au [100], with work function 5.47 eV. Consistent with the reported study of GNRFET, it has a high on-off ratio. Also the transfer curve is consistent with the reported results available in the literature [36,40].

3.1. Detection of the presence of biomolecules

In this subsection, the action of the biosensor to realize the presence of biomolecules in the solution will be discussed. To elaborate, an analyte solution containing the biomolecules (BMO) that is to be determined has been considered to be introduced to the sensor on the surface of the top gate (a similar solution without the BMO has been provided on the surface of the bottom gate to confirm that the effects of only biomolecule absorption are being introduced). To reduce the complexity, it has been assumed that the BMOs will be absorbed on the top gate surface effectively without the use of any catalyst.

The adsorption of biomolecules on the gold surface is a chemi-absorption process where a dipole layer is created between the biomolecule layer and the metal surface. Separation between the monolayer BMO and the gate metal surface effects the gate work function change significantly and is well-established in the literature [28,29].

In general, an adsorbate layer is involved in charge transfer in the adsorption reaction and induces the observable change in the work function of the metal surface. As, electron leaving the metal must pass through the interface diploes layer- created as a result of charge transfer. Depending on the orientation of the dipole, this can either make removing the electron easy or difficult. So, it is the dipole moment that determines whether the effect of adsorption on the top gate will increase or decrease the work function of the metal. The above process is realized by the change in electron density of the metal surface. The

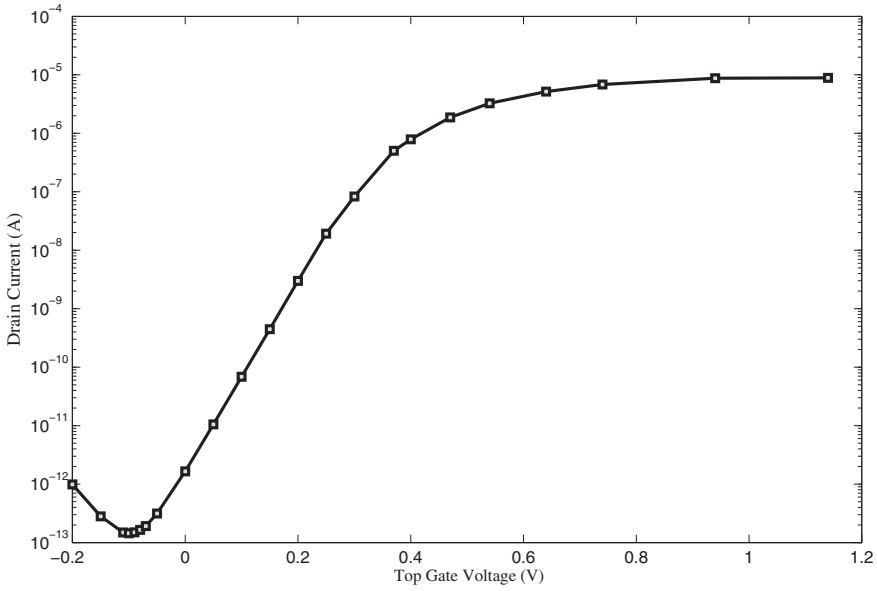

Fig. 2. Reference transfer curve of the GNRFET for the purpose of the biosensor; simulated without the analyte solution on the top and the bottom gate. The impressive on-off ratio makes it a suitable basis device in biosensor application.

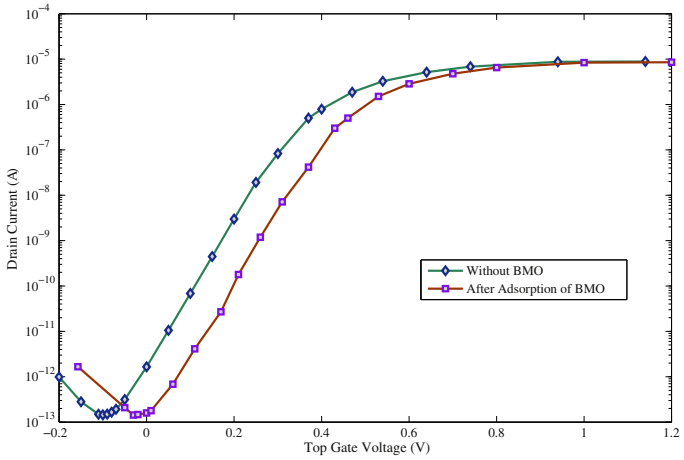

(a)

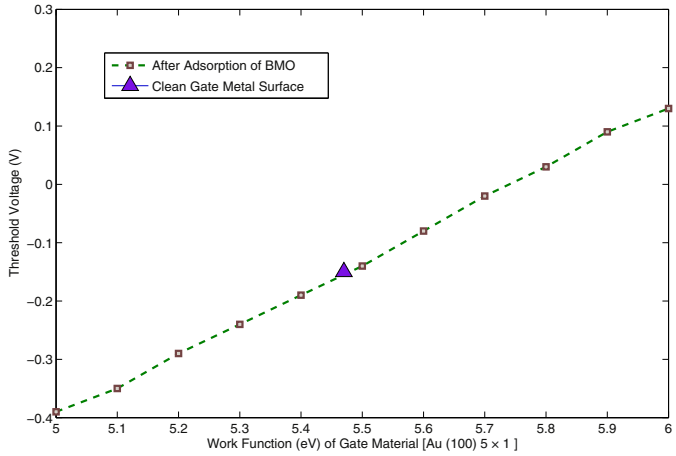

(b)

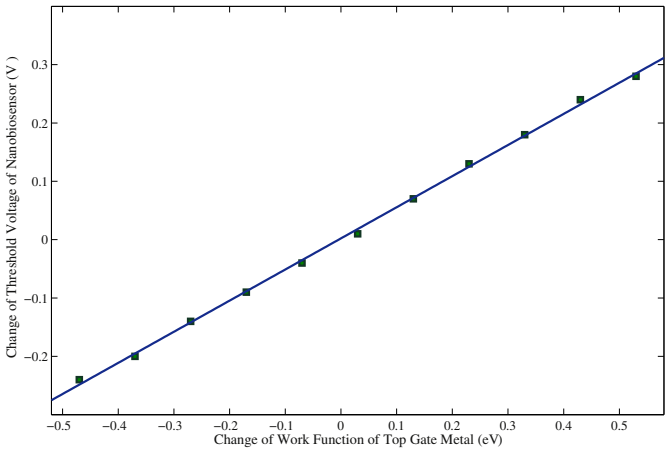

(c)

Fig. 3. (a) Shifting of Threshold Voltage due to adsorption of the biomolecule on top gate material, Au (100) (5 × 1). (b) As more and more biomolecules are adsorbed, the threshold voltage of the nanobiosensor continues to shift from the point obtained for clean metal surface, for both increase and decrease of the work function of the top gate material. (c) A linear relationship exists between the change of threshold voltage and change of work function of the top gate material of the nanobiosensor.

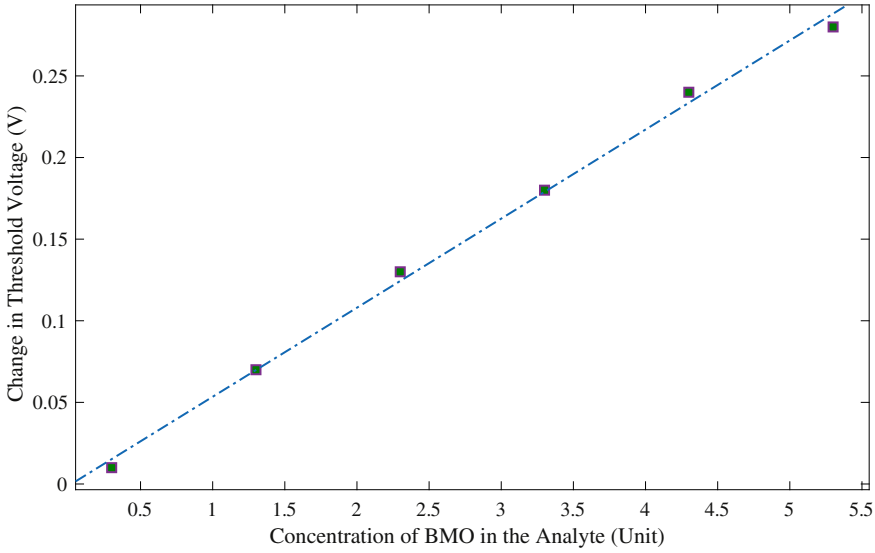

Fig. 4. The amount of change in threshold voltage of the nanobiosensor is linearly related to the concentration of the adsorption (the amount of biomolecule adsorbed in the top gate material). As more and more biomolecules are adsorbed, the amount of interface dipole on the gate material increases and it corresponds to the change in the threshold voltage of the nanobiosensor.

effect of adsorption i.e. interface dipole results in change in work function ($\Delta\varnothing_G$) as [28],

$$e\Delta\mu = \Delta\varnothing_G\, \varepsilon_0 A \tag{1}$$

where A = surface area per molecule, ε_0 = lowest occupied molecular orbital or LUMO energy, $\Delta\mu$ = change in interface dipoles.

From Fig. 3(a), it is seen that when the electro statistics of the sensor is simulated incorporating the change (increase) of work function, there exist a shifting of the drain current when plotted as a function of the gate voltage. To be more exact the threshold voltage has shifted towards the right of the axis. The threshold voltage has been defined as the applied gate voltage required to achieve the positive slope of the I_D-V_{GS} characteristic curve. This change in the threshold voltage will determine the presence of the biomolecules in the analyte. This shifting can be further expanded to create a calibration curve of Fig. 3(c). Fig. 3(b) relates the change of threshold voltages that the nanobiosensor experience with the change the gate material Au [100] undergoes due to absorption of biomolecules on the surface. This relationship is linear. This will be further explored in the following subsection. For simulation purpose, the amount of adsorbed peptides from the analyte on the top gate material that result in a change of 0.1 eV in the work function of the top gate material is considered to be 1 unit of biomolecular concentration in the aqueous solution. This relationship of threshold voltage change in response to the increasing concentration is presented in Fig. 4.

3.2. Analytical model

Starting from the fact that a positive net fixed charge density usually exists in the oxide layer and that results in the oxide capacitance. For zero applied gate voltage, $V_{OX0} + \varnothing_{S0} = -\varnothing_{GS}$. The voltage V_{OX0} is the potential drop across the oxide for zero applied gate voltage and potential $\varnothing_{S0}$ is the surface potential for same case. The right-hand term represents the difference of work function for gold and Graphene Nano-Ribbon. The potential drop across the oxide and the surface potential will change whenever a gate voltage is applied. So, it can then be written,

$$\begin{aligned} V_G &= \Delta V_{OX} + \Delta\varnothing_S = (V_{OX} - V_{OX0}) + (\varnothing_S - \varnothing_{S0}) \\ V_{GS} &= \varnothing_S + V_{OXT} + \varnothing_{GS} \end{aligned} \tag{2}$$

where V_{OXT} represents the voltage across the oxide at this threshold inversion point. It is related to the charge on the metal and to the oxide capacitance,

$$V_{OXT} = \frac{\text{Charge on the metal } (q_m)}{\text{capacitance of the oxide } (Cox)}$$

After the adsorption of BMO on the top gate

$$V_{GS,eff} = \varnothing_S + V_{OXT}' + \varnothing_{GS}' \tag{3}$$

$$\begin{aligned} \text{So, } \Delta V_{GS} &= V_{GS,eff} - V_{GS} \\ &= \Delta V_{OXT} + \Delta\varnothing_G \\ &= \frac{\Delta q_m}{Cox} + \frac{e\Delta\mu}{\varepsilon_0 A} \text{[Using the eq. (1)]} \end{aligned} \tag{4}$$

For a GNRFET a compact model is developed [41] and the current density is given by.

$$I = \frac{W}{L}\frac{e\,u\int_0^{V_{ds}}(n)\,dV}{1+\frac{u\,V_{ds}}{L\,v_{sat}}} \tag{5}$$

where carrier concentration,

$$n = \sqrt{n_0^2 + (C_{ox}(V_{GS} - V(x) - V_0)/e)^2} \tag{6}$$

n_0 is the minimum sheet carrier concentration, u is the low field mobility and v_{sat} is the saturation velocity.

The effect of adsorption of BMO on the gate surface is modeled as the change in effective gate voltage. It is found that this effective gate voltage results in change of carrier concentration in the nanobiosensor. Using 3, 4 and 6, total carrier concentration of the nanobiosensor after adsorption of BMO is found as,

$$n_{total} = \sqrt{n^2 + n_{BMO}}$$

where

$$n_{BMO} = \frac{(\Delta q_m + C_{ox}\,\Delta\varnothing_G)^2}{e^2} \tag{7}$$

So, the primary result of interface dipole in the biosensor is that it enforces a change (increase or decrease depending on the dipole moment) in the carrier concentration of the FET.

So, after the biomolecules have been introduced to the top gate the drain current of the FET will be, $I = \frac{W}{L}\frac{e\,u\int_0^{V_{ds}}(\sqrt{n^2+n_{BMO}})\,dV}{1+\frac{u\,V_{ds}}{L\,v_{sat.}}}$

In terms of the threshold voltage Eq. (3) changes to $V_{TH} = \varnothing_S + V_{OXT}' + \varnothing_{GS}'$.

Now in the proposed nanobiosensor, absorption of biomolecules on the metal gate changes the charge density of the metal due to pillow effect [28] and the work function of the metal (increase). The effect is twofold; change of the gold-semiconductor (Graphene nanoribbon) work function difference$\varnothing_{GS}$ and change in the parameter V_{OXT}. The resultant effect on the threshold voltage though linear but not proportionate to the change in work function of gate metal.

Now, the current sensitivity of the nanobiosensor for 1 unit of biomolecules in the analyte is calculated using the equation,

$$S = \frac{|I_{BMO} - I_{WBMO}|}{I_{WBMO}} \times 100\%$$

where I_{BMO} and I_{WBMO} is the current after and before the biomolecule adsorption on the gate metal respectively. As seen from Fig. 3, the relative change in the "on" current of the sensor for the introduction of BMO is quite small compared to the change of the same in the sub-threshold region. This is because the on current is set to such a high value that small change in the drain current is not so significant. The effective gate voltage changes due to the change of work function for adsorption of biomolecules on gate material. This causes a relatively small change to the "on" current of the nanobiosensor. On the other hand, in the sub-threshold regime, the device conducts small or almost no current. And so, the drain current results in significant changes after introduction of BMO. As a result, in Fig. 5, high sensitivity has been observed for lower values of the top gate voltage and the current sensitivity of the sensor decreases rapidly as the device changes from sub-threshold region to on state. BioFETs with high sensitivity is essential to increase the detection limit. The calculated high sensitivity of nanobiosensor points to its potentiality to contribute towards detection at an early stage. The current sensitivity, S can be realized from the following equation also:

$$S = a\ \exp(b * V_{GS})$$

where the fitting parameters $a = 1.53 \times 10^4$ and $b = -6.56$

This finding leads to the understanding that the operation of the FET as a nanobiosensor in the sub-threshold region provides more precise results as well as increases the smallest amount that can be detected.

The sensitivity of the nanobiosensor is characterized in terms of the amount of the threshold voltage shift per each unit of biomolecular adsorption on the top gate of the device. Whereas the lowest limit that can be detected using the simulation is the lowest amount of threshold voltage shift that can be measured by the external circuit in event of a biomolecular adsorption.

Lowest limit of detection (Using simulation): 0.03 V change in the threshold value.

Sensitivity: 0.05 V in terms of threshold voltage change per unit adsorption of biomolecules.

On-Off ratio: 10^4

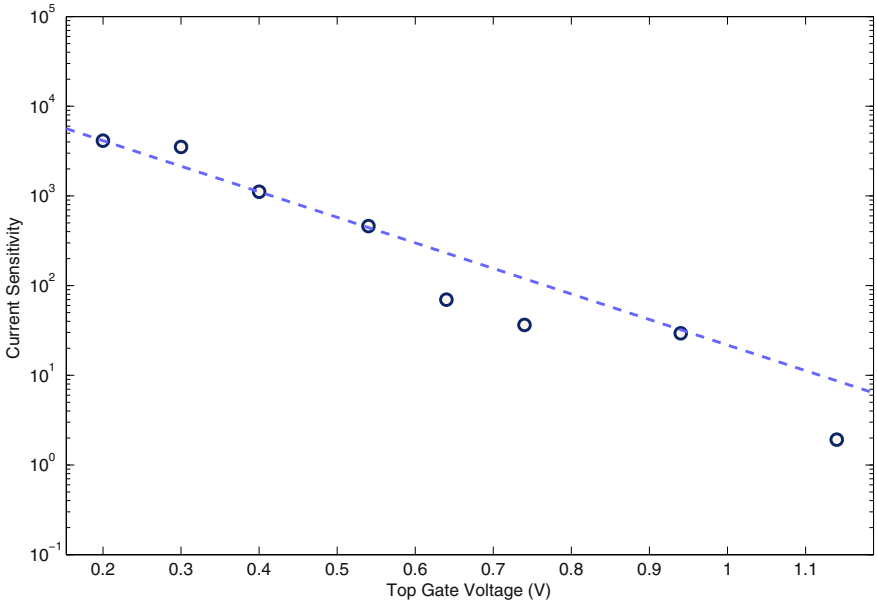

Fig. 5. Current sensitivity of the nanobiosensor as a function of the top gate voltage for adsorption of BMO that results in 0.1 eV work function change of gate material. Very high sensitivity has been found in the sub-threshold region.

3.3. Aqueous concentration of biomolecules

In this subsection, the study is further extended whereby detecting the amount of change in the threshold voltage; the concentration of the biomolecules in the analyte can be determined. For the stated purpose, the work of Langmuir will be related to this context.

The Langmuir Isotherm, developed in 1916, describes the adsorption of molecules on a solid surface. It relates the concentration of the medium above the solid at a fixed temperature to the amount of adsorption that has occurred. The Langmuir equation is given by,

$$\Gamma = \Gamma_{\max} \frac{K\,C}{1 + K\,C}$$

where 'K' is the Langmuir Constant, 'C' is the aqueous concentration, 'Γ' is the amount adsorbed and 'Γ_{max}' is the maximum amount adsorbed as 'C' increases.

Therefore this 'Γ' in Langmuir's Equation corresponds to the number of dipoles created at the metal-organic interface, which in turn is directly proportional to the change in work function of the clean metal surface. As a result, the 'Γ' in Langmuir's Equation can be represented by the change in work function.

In order to find the concentration of the biomolecule present in the aqueous solution, it is first needed to determine the 'Γ_{max}'. This can be executed by first introducing the GNRFET to the solution containing the said biomolecule at very high concentration. This is to ensure that all the sites available for adsorption on the Gate metal surface are occupied with biomolecules. The change in work function, '$\Delta\varnothing_{G\max}$' in this instant is determined from the calibration curve of Fig. 3(c). This will correspond to the 'Γ_{max}' in Langmuir equation. After this, the solution, whose concentration is to be calculated is introduced to the GNRFET. Since change in dipole is directly proportional to change in work function and number of molecules adsorbed is actually the number of interface dipoles created, thus it can be said that, $\Gamma \propto \Delta\varnothing_G$. Again, the change in work function, '$\Delta\varnothing_G$', which represents the 'Γ', is determined similarly using the above procedure. Therefore,

$$\frac{\Gamma}{\Gamma\max} = \frac{\Delta\varnothing_G}{\Delta\varnothing_G\max} = \frac{K\,C}{1 + K\,C}$$

Some simple rearrangements lead to the following,

$$C = \frac{\Delta\varnothing_G}{K\,(\Delta\varnothing_{G_{max}} - \Delta\varnothing_G)}$$

Given that Langmuir Constant is known, the unknown aqueous concentration C can be calculated from the above relationship.

4. Conclusion

In this study, adsorption based nanobiosensor using graphene nanoribbon field effect transistor has been delineated. The extensive features of graphene nanoribbon pave the way for the idea of precipitous detection of biomolecules. Moreover, gold [Au (100)] provides fine chemisorption of biomolecule which also provides a way for elimination of bio-receptors. The adsorption results in a significant detectable change in threshold voltage of the FET. As a result, the presence of biomolecule can be detected through the shifting of the transfer curve of the nanobiosensor. Furthermore, the nanobiosensor shows excellent sensitivity in the subthreshold region. Due to the introduction of biomolecules, the change of threshold voltage of the FET in accordance with the change of interface dipoles at the gate metal leads to a possible calculation of the aqueous concentration of the biomolecules. Application of this FET as a biosensor can be further extended to the detection of other biomolecules like DNA, Amino acids, Azo-derivatives etc. As new processes and catalysts to make efficient adsorption of biomolecules on metal surface continue to flourish, this graphene-based nanobiosensor should be a promising candidate for future biosensing application.

References

[1] K.S. Novoselov, A.K. Geim, S.V. Morozov, D. Jiang, Y. Zhang, S.V. Dubonos, I.V. Grigorieva, A.A. Firsov, Electric field effect in atomically thin carbon films, Science 306 (5696) (22 Oct 2004) 666–669, http://dx.doi.org/10.1126/science.1102896.

[2] Qing Hua Wang, Kourosh Kalantar-Zadeh, Andras Kis, Jonathan N. Coleman, Michael S. Strano, Electronics and optoelectronics of two-dimensional transition metal dichalcogenides, Nat. Nanotechnol. 7 (2012) 699–712, http://dx.doi.org/10.1038/nnano.2012.193.

[3] Celine I.L. Justino, Ana R. Gomes, Ana C. Freitas, Armando C. Duarte, Teresa A.P. Rocha-Santos, Graphene based sensors and biosensors, TrAC Trends Anal. Chem. 91 (June 2017) 53–66.

[4] Yasuhide Ohno, Kenzo Maehashi, Kazuhiko Matsumoto, Label-free biosensors based on aptamer-modified graphene field-effect transistors, J. Am. Chem. Soc. 132 (51) (2010) 18012–18013, http://dx.doi.org/10.1021/ja108127r.

[5] YueCui PratimaLabroo, Graphene nano-ink biosensor arrays on a microfluidic paper for multiplexed detection of metabolites, Anal. Chim. Acta 813 (27) (February 2014) 90–96.
[6] L. Wu, H.S. Chu, W.S. Koh, E.P. Li, Highly sensitive graphene biosensors based on surface plasmon resonance, Opt. Express 18 (14) (2010) 14395–14400, http://dx.doi.org/10.1364/OE.18.014395.
[7] Y. Zhang, et al., Single-layer transition-metal dichalcogenide nanosheet-based nanosensors for rapid, sensitive, and multiplexed detection of DNA, Adv. Mater. 27 (5) (2015) 935–939.
[8] Martin Pumera, Adeline Huiling Loo, Layered transition-metal dichalcogenides (MoS2 and WS2) for sensing and biosensing, TrAC Trends Anal. Chem. 61 (October 2014) 49–53.
[9] C. Berger, Z. Song, T. Li, X. Li, A.Y. Ogbazghi, R. Feng, Z. Dai, A.N. Marchenkov, Ultrathin epitaxial graphite: 2D electron gas properties and a route toward graphene-based nanoelectronics, J. Phys. Chem. B 108 (52) (2004) 19912–19916.
[10] Cedric Sire, Florence Ardiaca, Sylvie Lepilliet, Jung-Woo T. Seo, Mark C. Hersam, Gilles Dambrine, Henri Happy, Vincent Derycke, Flexible gigahertz transistors derived from solution-based single layer graphene, Nano Lett. 12 (2012) 1184–1188.
[11] Parshant Sharma, Vijit Mangla, Rahul Dhyani, The zero band gap semiconductor: graphene, Int. J. Innov. Res. Technol. 1 (6) (2014) 1886–1888.
[12] Mihir Choudhury, Youngki Yoon, Jing Guo, Kartik Mohanram, Technology exploration for graphene nanoribbon FETs, DAC '08 Proceedings of the 45th annual Design Automation Conference, 2008, pp. 272–277.
[13] Melinda Y. Han, Barbaros Özyilmaz, Yuanbo Zhang, Philip Kim, Energy band-gap engineering of graphene nanoribbons, Phys. Rev. Lett. 98 (2007) 206805, , http://dx.doi.org/10.1103/PhysRevLett.98.206805.
[14] A.K. Geim, K.S. Novoselov, The rise of graphene, Nat. Mater. 6 (2007) 183–191, http://dx.doi.org/10.1038/nmat1849.
[15] L. Tang, et al., Preparation, structure, and electrochemical properties of reduced graphene sheet films, Adv. Mater. 27 (5) (2015) 935–939 (Melinda Y. Han, Barbaros Özyilmaz, Yuanbo Zhang, and Philip Kim Advanced Functional Materials Volume 19, Issue 17, 2009 Pages 2782–2789).
[16] L.H. Hess, M.V. Hauf, M. Seifert, F. Speck, T. Seyller, M. Stutzmann, I.D. Sharp, J.A. Garrido, High-transconductance graphene solution-gated field effect transistors, Appl. Phys. Lett. 99 (2011) 033503, , http://dx.doi.org/10.1063/1.3614445.
[17] Yasuhide Ohno, Kenzo Maehashi, Yusuke Yamashiro, Kazuhiko Matsumoto, Electrolyte-gated graphene field-effect transistors for detecting pH and protein adsorption, Nano Lett. 9 (9) (2009) 3318–3322, http://dx.doi.org/10.1021/nl901596m.
[18] Nihar Mohanty, Vikas Berry, Graphene-based single-bacterium resolution biodevice and DNA transistor: interfacing graphene derivatives with nanoscale and microscale biocomponents, Nano Lett. 8 (12) (2008) 4469–4476, http://dx.doi.org/10.1021/nl802412n.
[19] Seon Joo Park, Oh. Seok Kwon, Sang Hun Lee, Hyun Seok Song, Tai Hyun Park, Jyongsik Jang, Ultrasensitive flexible graphene based field-effect transistor (FET)-type bioelectronic nose, Nano Lett. 12 (10) (2012) 5082–5090, http://dx.doi.org/10.1021/nl301714x.
[20] Jieyi Zhu, Fuzhou Niu, Changan Zhu, Jie Yang, Ning Xi, Graphene-based FET detector for E. coli K12 real-time monitoring and its theoretical analysis, J. Sensors (2016) 4641398, , http://dx.doi.org/10.1155/2016/4641398.
[21] B.L. Allen, P.D. Kichambare, A. Star, Carbon nanotube field-effect-transistor-based biosensors, Adv. Mater. 19 (11) (2007) 1439–1451, http://dx.doi.org/10.1002/adma.200602043.
[22] A. Errachid, N. Zine, J. Samitier, J. Bausells, Fet-based chemical sensor systems fabricated with standard technologies, Electroanalysis 16 (22) (2004) 1843–1851.
[23] Yijian Ouyang, Modeling and Simulation of Graphene Nanoribbon Electronics, University of Florida, 2011.
[24] L. Jiao, L. Zhang, X. Wang, G. Diankov, H. Dai, Narrow graphene nanoribbons from carbon nanotubes, Nature 458 (7240) (Apr. 2009) 877–880.
[25] Y. Sui, J. Appenzeller, Screening and interlayer coupling in multilayer graphene field-effect transistors, Nano Lett. 9 (8) (2009) 2973–2977.
[26] Michio Tokuyama, Tatsuo Moriki, Yuto Kimura, Self-diffusion of biomolecules in solution, Phys. Rev. E 83 (16 May 2011) 051402Published.
[27] Dominique Costa, Letizia Savio, Claire-Marie Pradier, Adsorption of amino-acids and peptides on metal and oxide surfaces in water environment: a synthetic and prospective review, J. Phys. Chem. B (2016), http://dx.doi.org/10.1021/acs.jpcb.6b05954.
[28] P.C. Rusu, G. Giovannetti, C. Weijtens, R. Coehoorn, G. Brocks, Work function pinning at metal-organic interfaces, J. Phys. Chem. C 113 (23) (2009).
[29] V.D. Renzi, R. Rousseau, D. Marchetto, R. Biagi, S. Scandolo, U.D. Pennino, Metal work-function changes induced by organic adsorbates: a combined experimental and theoretical study, Phys. Rev. Lett. 95 (4) (2005), http://dx.doi.org/10.1103/physrevlett.95.046804.
[30] Z.E. Hughes, L.B. Wright, T.R. Walsh, Biomolecular adsorption at aqueous silver interfaces: first-principles calculations, polarizable force-field simulations, and comparisons with gold, Langmuir 29 (43) (2013 Oct 29) 13217–13229, http://dx.doi.org/10.1021/la402839q (Epub 2013 Oct 14).
[31] B. Louise, P. Mark Rodger Wright, Stefano Corni, Tiffany R. Walsh, GolP-CHARMM: first-principles based force fields for the interaction of proteins with Au(111) and Au(100), J. Chem. Theory Comput. 9 (2013) 1616–1630.
[32] Louise Wright, P. Mark Rodger, R. Walsh Tiffany, Stefano Corni, First-principles-based force field for the interaction of proteins with Au(100)(5 × 1): an extension of GolP-CHARMM, J. Phys. Chem. C 117 (2013) 24292–24306, http://dx.doi.org/10.1021/jp4061329.
[33] K.S. Novoselov, Electric field effect in atomically thin carbon films, Science 306 (5696) (2004) 666–669, http://dx.doi.org/10.26/science.1102896.
[34] D. Gunlycke, H.M. Lawler, C.T. White, Room-temperature ballistic transport in narrow graphene strips, Phys. Rev. B 75 (8) (2007), http://dx.doi.org/10.1103/physrevb.75.085418.
[35] Yijian Ouyang Hongjie Dai Jing Guo, Projected performance advantage of multilayer graphene nanoribbons as a transistor channel material, J. Nano Res. 3 (1) (January 2010).
[36] G. Fiori, G. Iannaccone, Simulation of graphene nanoribbon field-effect transistors, IEEE Electron Device Lett. 28 (8) (2007) 760–762.
[37] Supriyo Datta, Nanoscale device modeling: the Green's function method, Superlattice. Microst. 28 (4) (2000), http://dx.doi.org/10.1006/spmi.2000.0920.
[38] A. Trellakis, A.T. Galick, A. Pacelli, U. Ravaioli, Iteration scheme for the solution of the two-dimensional Schrödinger–Poisson equations in quantum structures, J. Appl. Phys. 81 (1997) 7800–7804.
[39] K. Alam, Transport and performance of a zero-Schottky barrier and doped contacts graphene nanoribbon transistor, Semicond. Sci. Technol. 24 (1) (2009) 015007.
[40] N. Akhavan, G. Jolley, G.U. Membreno, J. Antoszewski, L. Faraone, Study of uniformly doped graphene nanoribbon transistor (GNR) FET using quantum simulation, Commad 2012, 2012, http://dx.doi.org/10.1109/commad.2012.6472363.
[41] Inanc Meric, Natalia Baklitskaya, Philip Kim, Kenneth L. Shepard, RF performance of top-gated, zero-bandgap graphene field-effect transistors, Proceedings of the IEEE International Electron Devices Meeting, December 2008, pp. 1–4 (San Francisco, Calif, USA).